The Conserved Active Site Proline Determines the Reducing Power of Staphylococcus aureus Thioredoxin

ARTICLE *in* JOURNAL OF MOLECULAR BIOLOGY · JUNE 2007

Impact Factor: 4.33 · DOI: 10.1016/j.jmb.2007.02.045 · Source: PubMed

9 AUTHORS, INCLUDING:

Goedele Roos
Vrije Universiteit Brussel
41 PUBLICATIONS **587** CITATIONS
SEE PROFILE

Khadija Wahni
Vrije Universiteit Brussel
18 PUBLICATIONS **274** CITATIONS
SEE PROFILE

Guy Vandenbussche
Université Libre de Bruxelles
37 PUBLICATIONS **961** CITATIONS
SEE PROFILE

Joris Messens
Vlaams Instituut voor Biotechnologie, Vrije …
76 PUBLICATIONS **2,277** CITATIONS
SEE PROFILE

doi:10.1016/j.jmb.2007.02.045 J. Mol. Biol. (2007) 368, 800–811

JMB

Available online at www.sciencedirect.com

ScienceDirect

ELSEVIER

The Conserved Active Site Proline Determines the Reducing Power of *Staphylococcus aureus* Thioredoxin

Goedele Roos[1,2,3,4], Abel Garcia-Pino[1,2], Karolien Van belle[1,2,3] Elke Brosens[1,2,3], Khadija Wahni[1,2,3], Guy Vandenbussche[5] Lode Wyns[1,2], Remy Loris[1,2] and Joris Messens[1,2,3]*

[1]*Department of Molecular and Cellular Interactions, VIB 1050 Brussel, Belgium*

[2]*Ultrastructure Laboratory Vrije Universiteit Brussel Belgium*

[3]*Brussels Center for Redox Biology†, Belgium*

[4]*Algemene Chemie, Vrije Universiteit Brussel, Belgium*

[5]*Centre de Biologie Structurale et de Bioinformatique, Structure et Fonction des Membranes Biologiques, Université Libre de Bruxelles, Brussel, Belgium*

**Corresponding author*

Nature uses thioredoxin-like folds in several disulfide bond oxidoreductases. Each of them has a typical active site Cys-X-X-Cys sequence motif, the hallmark of thioredoxin being Trp-Cys-Gly-Pro-Cys. The intriguing role of the highly conserved proline in the ubiquitous reducing agent thioredoxin was studied by site-specific mutagenesis of *Staphylococcus aureus* thioredoxin (Sa_Trx). We present X-ray structures, redox potential, pK_a, steady-state kinetic parameters, and thermodynamic stabilities. By replacing the central proline to a threonine/serine, no extra hydrogen bonds with the sulphur of the nucleophilic cysteine are introduced. The only structural difference is that the immediate chemical surrounding of the nucleophilic cysteine becomes more hydrophilic. The pK_a value of the nucleophilic cysteine decreases with approximately one pH unit and its redox potential increases with 30 mV. Thioredoxin becomes more oxidizing and the efficiency to catalyse substrate reduction (k_{cat}/K_M) decreases sevenfold relative to wild-type Sa_Trx. The oxidized form of wild-type Sa_Trx is far more stable than the reduced form over the whole temperature range. The driving force to reduce substrate proteins is the relative stability of the oxidized *versus* the reduced form $\Delta(T_{1/2})_{ox/red}$. This driving force is decreased in the Sa_Trx P31T mutant. $\Delta(T_{1/2})_{ox/red}$ drops from 15.5 °C (wild-type) to 5.8 °C (P31T mutant). In conclusion, the active site proline in thioredoxin determines the driving potential for substrate reduction.

Keywords: structure; kinetics; pK_a; redox potential; stability

Introduction

Nature alters existing folds slightly to make that proteins adopt new roles. The role or function of a protein is determined by its essential structural elements, which are found conserved within the same protein present in many organisms. Here, we look at the reduction power of thioredoxin. Thioredoxins reduce disulfide bonds in proteins quickly. For example, thioredoxin from *Escherichia coli* (Ec_Trx) reduces the disulfide bonds of insulin 10^4-fold faster than dithiothreitol does.[1] Its function has been implicated in many pathways and it provides a protective role against many different types of damaging stresses.[2,3]

Thioredoxin is a small, 12 kDa protein found in all living cells from archaea to humans. The structures of both the oxidized and reduced form of Ec_Trx were solved by NMR.[4] In the PDB‡, the reduced

†http://redox.vub.ac.be/

Present address: J. Messens, Ultrastructure Laboratory, Vrije Universiteit Brussel, Pleinlaan 2, 1050 Brussel, Belgium.

Abbreviations used: Sa_Trx, thioredoxin from *Staphylococcus aureus*; Ec_Trx, thioredoxin from *Escherichia coli*; GSH, reduced glutathione; GSSG, oxidized glutathione; Grx, glutaredoxin; r.m.s.d., root-mean-square deviation; DSC, differential scanning calorimetry.

E-mail address of the corresponding author: joris.messens@vub.ac.be

‡http://www.rcsb.org/pdb/home/home.do

Table 1. Data collection and refinement statistics of Sa_Trx

	Wild-type	P31T	P31S	P31TC32S
Resolution limits (Å)	15.0–2.2 (2.3–2.2)	15.0–2.2 (2.3–2.2)	15.0–2.4 (2.5–2.4)	15.0–2.55 (2.65–2.55)
Space group	$P2_12_12_1$	$P2_12_12_1$	$P2_12_12_1$	$P2_12_12_1$
Unit cell (Å)	$a=41.0$	$a=41.7$	$a=41.2$	$a=41.3$
	$b=49.7$	$b=49.5$	$b=49.6$	$b=49.2$
	$c=54.5$	$c=55.6$	$c=54.8$	$c=54.9$
Wavelength (Å)	0.812	0.918	0.813	0.934
Measured reflections	43,223 (3076)	29,248 (2788)	18,019 (1806)	14,609 (1378)
Unique reflections	6123 (587)	6140 (590)	4694 (464)	3928 (376)
Completeness (%)	97.7 (98.5)	99.4 (99.0)	99.7 (99.6)	99.4 (99.2)
R_{merge}	0.093 (0.449)	0.058 (0.431)	0.071 (0.311)	0.094 (0.454)
I/σ_I	14.8 (4.3)	16.89 (4.2)	13.17 (4.3)	9.85 (3.5)
Refinement statistics				
R_{cryst}/R_{free}	0.203/0.249	0.196/0.246	0.193/259	0.202/0.255
Ramachandran profile				
Core (%)	86.7	92.3	90.1	89.9
Allowed (%)	12.2	7.7	9.9	11.0
Disallowed (%)	1.1	0	0	0
r.m.s. deviation bonds (Å)	0.006	0.006	0.007	0.007
r.m.s. angles (°)	1.305	1.359	1.324	1.344
Number of water molecules	22	40	11	0
PDB entry	2O7K	2O85	2O87	2O89

Values between parentheses correspond to the highest resolution shell. $R_{merge}=(\sum_{hkl}r|I_{hkl}-<I>|)/\sum_{hkl}I$.

form of thioredoxin is always a solution structure. Many X-ray structures in the oxidized state exist. All thioredoxins have similar three-dimensional structures comprising a central core of five β-strands surrounded by four α-helices. All feature a conserved active-site loop containing two redox-active cysteine residues in the sequence Trp-Cys-Gly-Pro-Cys.[5] The oxidized form, thioredoxin-S_2, contains a disulfide bridge between those two cysteine residues that is reduced to a dithiol by the NADPH-dependent flavoprotein, thioredoxin reductase. The reduced form, thioredoxin-$(SH)_2$, is a powerful and general protein disulfide bond oxidoreductase, with a redox potential of −268 mV for Sa_Trx[6] and −270 mV for Ec_Trx.[7] For comparison, DsbA, which is the strongest natural oxidant, has a redox potential of −119 mV.[8]

The pK_a value of the N-terminal cysteine of Ec_Trx (~7) is significantly lower compared to the pK_a of a cysteine in the absence of a structured protein environment (~8.3).[9–11] This low pK_a enables thioredoxin to act as a nucleophile and to attack disulfides in proteins. Thioredoxin catalyses the reduction of many exposed disulfides in proteins[12] such as ribonucleotide reductase, insulin, methionine sulfoxide reductase,[13] and *Staphylococcus aureus* pI258 arsenate reductase.[14]

The SWISSPROT database[15] harbours 97 thioredoxin sequences (Figure 1(a)). Some of these proteins have an overall sequence identity lower than 30% as compared to Sa_Trx, but even then the DF∗A∗WCGPC active site motif is highly conserved (Figure 1(a) and (b)). Next to the active site cysteine residues are a proline and a tryptophan highly conserved. This trypthophan is also present in the Trx-like domains of protein disulfide isomerase (PDI)[16] and of phosphoinositide-specific phospholipase C.[17] In two other members of the thioredoxin superfamily, DsbA and glutaredoxin, the CXXC-preceding tryptophan is absent (Figure 1(b)).

Here we investigate the role of the active site proline in Sa_Trx. We mutated the active site proline and solved the crystal structures of wild-type and Sa_Trx mutants (P31T, P31S, and P31TC32S) (Table 1). The redox potential, pK_a of the active site cysteine residues, the reducing activity, and the thermodynamic stability of these mutants are determined. Based on these results, we have qualified the presence of a proline in the active site of this ubiquitous reducing agent.

Results

The X-ray structures of Sa_Trx

Sa_Trx in its oxidized state displays the expected thioredoxin fold consisting of a central core of five β-strands enclosed by four α-helices (Figure 2). It is structurally most similar to the corresponding *E. coli* enzyme (PDB entry 2TRX), with an r.m.s.d. of 0.9 Å for 95 superimposable C^{α} atoms.[18] The active site containing Trp28-Cys29-Gly30-Pro31-Cys32 is located on the surface of the protein. In the oxidized form, the disulfide bond between residues 29 and 32 is oriented towards the interior of the molecule. This active site disulfide is located at the amino end of the α2-helix in a short segment that is separated from the rest of the helix by a kink due to the presence of a proline 37. Behind the disulfide, a conserved Pro73 is located, which is typically in *cis* conformation (Figure 2). Further, the conserved positive charge,

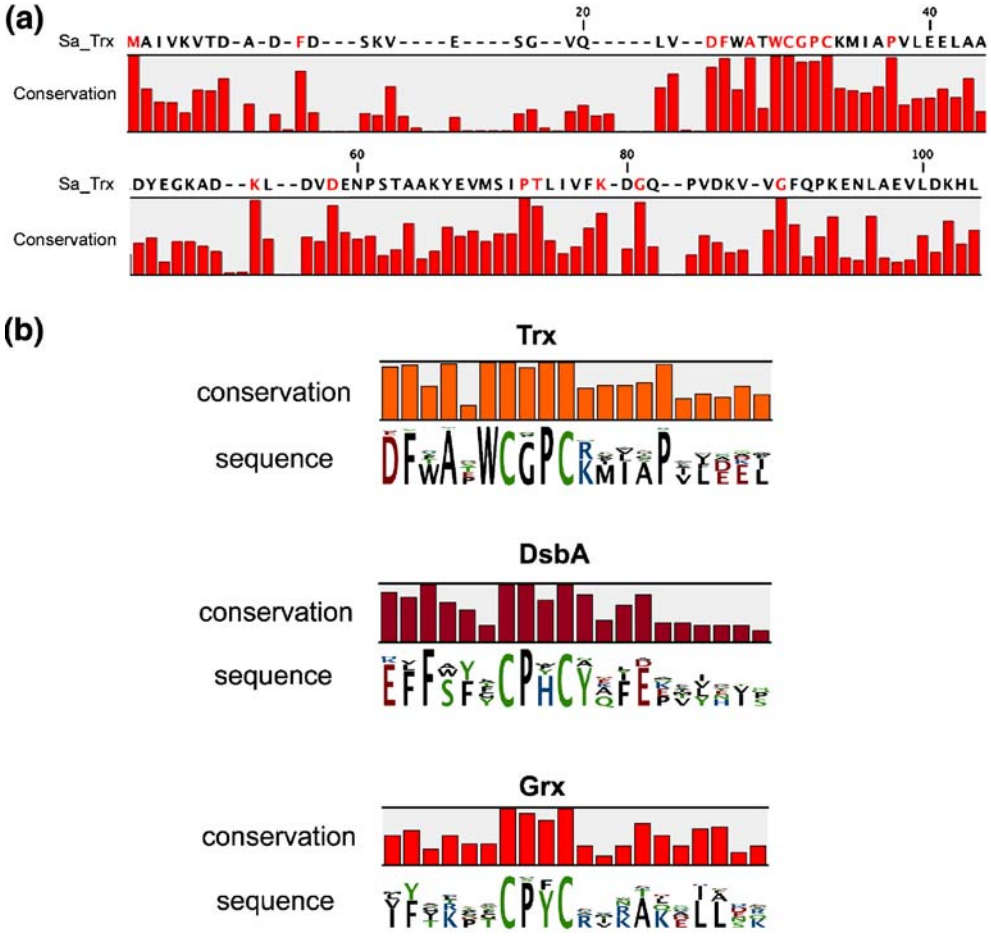

Figure 1. Sequence conservation in thioredoxin family. (a) Active site proline and tryptophan are highly conserved in thioredoxin. The multiple sequence alignment was computed with the program BLASTP (BLOSUM62 as matrix) with the complete Sa_Trx sequence as entry in the SWISSPROT database and resulted in 103 sequences, for which 97 are thioredoxins. The amount of conservation was plotted for each residue and the highly conserved residues are indicated in red. (b) The active site tryptophan is absent in DsbA and glutaredoxin (Grx). Comparison of the conservation of the active site in Trx, DsbA and Grx within the SWISSPROT database. The size of the amino acid single-letter code is proportional to the occurrence of that amino acid at each position. Graphs were made with CLC Protein Workbench 2.0.2. [http://www.clcbio.com/].

often present in the form of an arginine in thioredoxins from other species, is in Sa_Trx a lysine (Sa_Trx: Lys33) (Figure 1(a)).

P31S and P31T are structurally conservative mutations (r.m.s.d. of 0.12 Å and 0.15 Å for P31T and P31S, respectively, for all 104 C^{α} atoms of Sa_Trx P31T and P31S on wild-type Sa_Trx). This is equivalent to what was observed for the proline to serine mutation in the *E. coli* enzyme.[19,20] In Sa_Trx, the C^{α} and the C^{β} atoms of Pro31, Ser31, and Thr31 in wild-type and the respective mutants are on exactly the same position. The hydroxyl groups of the Ser31 (O^{γ}) and Thr31 ($O^{\gamma 1}$) are pointing in the opposite direction in their respective structures. Only the O^{γ} of Ser31 is in contact with the C^{δ} of Pro73 (2.9 Å); Thr31 has no contacting neighbours.

As it was not possible to reduce Sa_Trx in the crystal or crystallize its reduced state, we determined the crystal structure of the double mutant P31T/C32S as a mimic of reduced Sa_Trx. Yet again, the C32S mutation is a conservative mutation that does not perturb globally nor locally the structure. Sa_Trx P31TC32S also contains the essential features observed in reduced Ec_Trx (PDB entry 1XOB)[4] (r.m.s.d. of 0.85 Å for 97 equivalent C^{α} atoms). The side-chains of Cys29 and Ser32 are oriented towards the interior of the protein, suggesting the need of a conformational change during its attack on a substrate protein.

The orientation of the SH group of Cys29 in the Sa_Trx P31TC32S mutant and the SH group of the nucleophilic cysteine in Ec_Trx is identically. The side-chain sulfur atom of Cys29 is tilted away from Ser32 to accommodate for the increase in the S–S distance that occurs upon reduction of the wild-type protein (Figure 3). No additional hydrogen bond is introduced between the backbone amides (Thr31, Ser32) and the nucleophilic cysteine 29 (Figure 3(b)). An important difference with wild-type Sa_Trx is that by replacing the proline by a threonine or serine, the environment of the nucleophilic Cys29 becomes more hydrophilic.

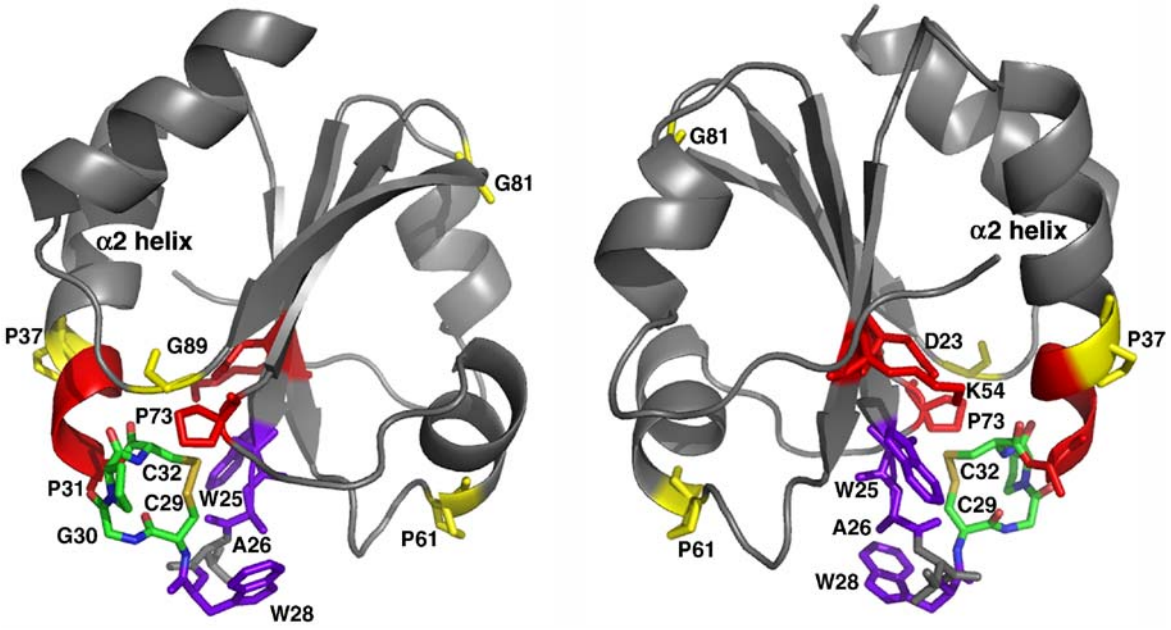

Figure 2. Sa_Trx has a typical thioredoxin fold. Ribbon diagram of the overall structure of Sa_Trx visualized from two different positions. The residues responsible for proper kinks (yellow), structure elements that influence the pK_a of the nucleophilic Cys29 (red), the conserved hydrophobic area (purple) and the CGPC active site motif (green atom type) are shown. The Figure was generated using MacPyMol (Delano Scientific LLC 2005).

The pK_a of the cysteine residues

Active site residues determine the pK_a of the nucleophilic cysteine in Sa_Trx (Table 2; Figure 4(a)). The pK_a values of the nucleophilic Cys29 and the buried Cys32 were determined by pH titration at 240 nm, since the thiolate ion has a higher absorption at this wavelength than the thiol group.[21] Compared to wild-type Sa_Trx (pK_a ~7.1), the pK_a of Cys29 decreases to 6.0 and 6.2 for the P31T and P31S mutants, respectively.

The influence of the C-terminal Cys32 (measured pK_a ~9) in WCGPC motif on the pK_a of the nucleophilic Cys29 was measured by replacing Cys32 with an alanine and a serine. Both Sa_Trx C32A and P31TC32S show an increase of the pK_a of 0.6 and 0.4 units relative to wild-type and Sa_P31T, respectively. As such, the C-terminal cysteine contributes in keeping the pK_a of the nucleophilic cysteine low.

The redox potential of the proline and tryptophan mutants

By replacing the active site proline 31 of the wild-type Sa_Trx by a threonine or a serine, Sa_Trx P31T/S becomes a more oxidizing enzyme. The redox potential increases (Table 2; Figure 4(b)). This observation is in line with a decrease of the pK_a of the nucleophilic Cys29 (*vide supra*).

The relative oxidizing power of P31S and P31T Sa_Trx was determined using glutathione as a standard. The glutathione redox scale compares the ability of proteins to transfer their disulfides to reduced glutathione.[22] The differential elution on reversed-phase chromatography of the oxidized and reduced forms of P31S and P31T Sa_Trx as function of $[GSH]^2/[GSSG]$ (i.e. E_h') allows the determination of the midpoint redox potential of the active-site disulfide (Cys29–Cys32). The molecular mass of the

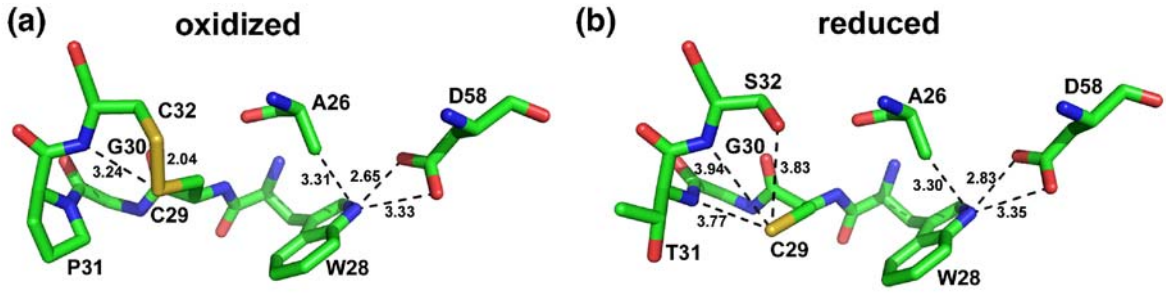

Figure 3. The active site of oxidized wild-type (a) and reduced P31TC32S (b) Sa_Trx are shown. The distances (Å) from S^{γ}Cys29 and $N^{\varepsilon 1}$Trp28 towards neighbour atoms are indicated. The Figure was generated using MacPyMol (Delano Scientific LLC 2005).

Table 2. pK_a and redox potential of Sa_Trx

Sa_Trx	pK_a Cys29	E' (mV)
P31T	6.0	−236
P31S	6.2	−244
P31TC32S	6.4	n.d.
Wild-type[6]	7.1	−268
C32A	7.7	n.d.

proteins associated to the two elution peaks was determined by mass spectrometry and showed a difference in 2 Da, consistent with the formation of a disulfide bridge between Cys32 and the nucleophilic Cys29.

Disulfide reducing activity of Sa_Trx mutants

Replacing the active site proline by a threonine or a serine in Sa_Trx decreases the efficiency of catalyis with a factor of seven (Table 3).

To determine Michaelis–Menten steady-state kinetic parameters of active site proline mutants, the reaction was followed indirectly by observing the rate of NADP formation.[6] The coupling enzyme in the cascade towards NADPH is thioredoxin reductase, delivering reducing equivalents to the oxidized thioredoxin. Previously, we have determined the conditions to ensure that thioredoxin reductase and NADPH are not rate limiting.[6] With oxidized pI258 arsenate reductase as the substrate, Sa_Trx P31T and P31S mutants display a specificity constant (k_{cat}/K_M) of 0.8×10^4 $M^{-1}s^{-1}$ (Table 3).

As oxidized thioredoxin itself has to be reduced by thioredoxine reductase in the cascade reaction, we analysed the oxidized Sa_Trx mutants as substrate.

Table 3. Kinetic parameters of thioredoxin and its active site proline mutants

Sa_Trx	K_M (μM)	k_{cat} (min^{-1})	k_{cat}/K_M ($M^{-1}s^{-1}$)
P31T	32	17	$0.9\ 10^4$

In the presence of an excess of oxidized P31T and P31S Sa_Trx (100 μM), we found that they are about twice as good a substrate for *S. aureus* thioredoxin reductase as oxidized wild type Sa_Trx.

Thermal stability

The presence of a proline in the active site of wild type Sa_Trx keeps the difference in stability between the oxidized and reduced form high (Figure 5(a)).

Differential scanning calorimetry (DSC) measurements are scan-rate independent for oxidized as well as reduced wild-type and P31T Sa_Trx (Figure 5(b)). All transitions show at least 90% reversibility. Furthermore, the ratio of calorimetric enthalpy (ΔH_c) and van't Hoff enthalpy (ΔH_{vh}), $\Delta H_c/\Delta H_{vh}$, is essentially one in all cases (Table 4). Insights into the nature of the structural changes upon Sa_Trx unfolding are provided by the model-dependent ΔH_{vh} and model-independent ΔH_c values. If both enthalpies are equal within the experimental error, then the observed transition proceeds in a two-state manner, i.e. the concentration of intermediates between the native and the unfolded state is negligibly small. This suggests a simple two-state equilibrium of a monomeric protein between a folded and an unfolded state.

Non-linear fitting of the two state unfolding model to the data provided the transition temperatures $T_{1/2}$

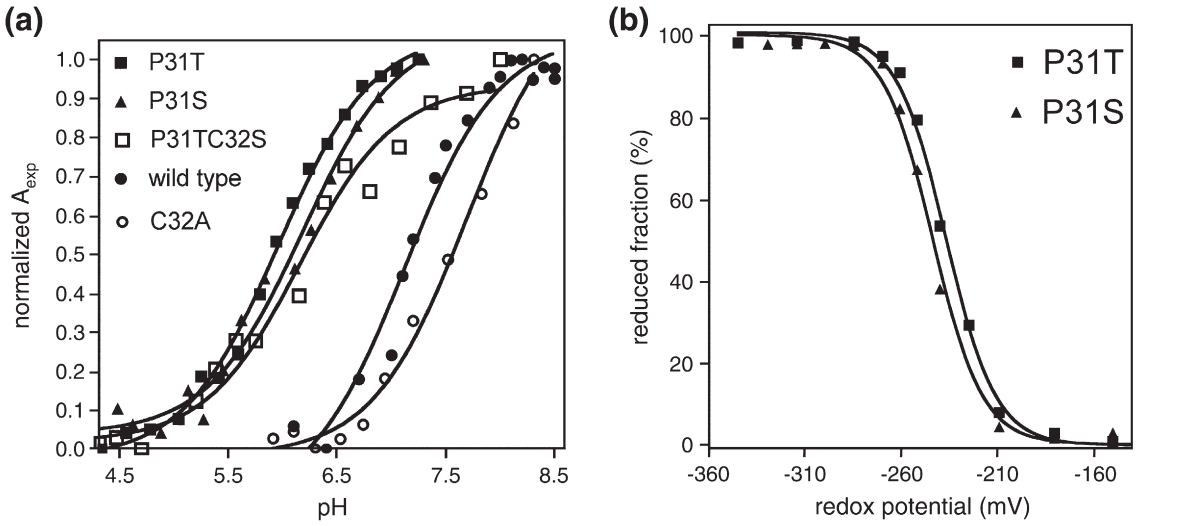

Figure 4. Titration curves for wild-type and the Sa_Trx mutants. (a) The pK_a of the nucleophilic cysteine. The specific absorption of the thiolate ion at 240 nm as function of the pH is shown. All data were fitted with the Henderson–Hasselbach equation. (b) Redox equilibrium with glutathione. Percentage of thioredoxin active site in the reduced form, calculated from the reversed-phase chromatographic profile after peak integration, as a function of redox potential are shown.

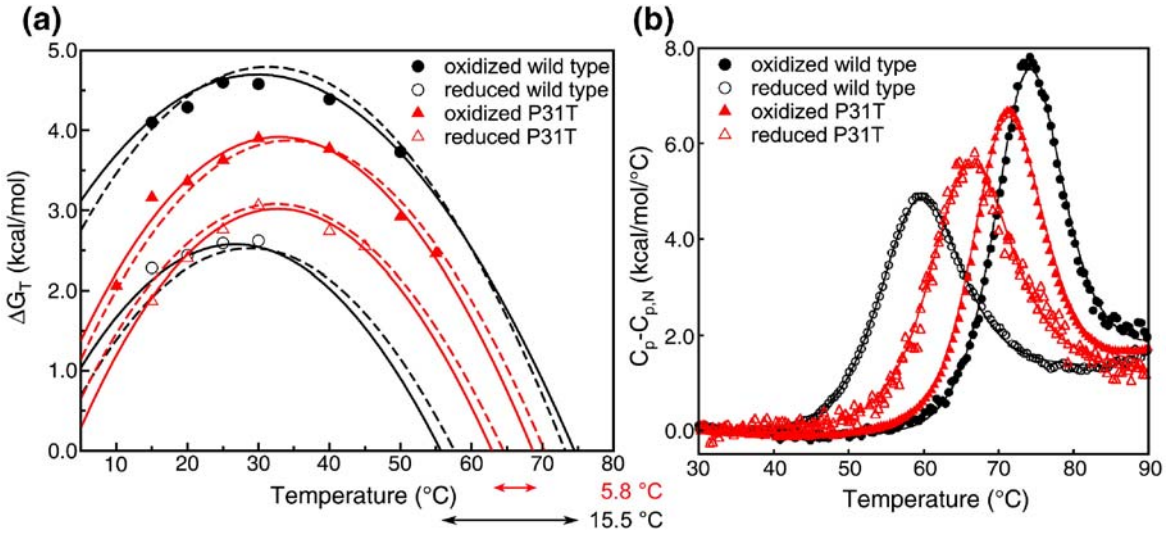

Figure 5. Thermodynamic stability of Sa_Trx. (a) Thermodynamic stabilities as function of temperature are shown for the oxidized (filled symbols) and reduced (open symbols) states of wild-type (black) and P31T (red). Curves were calculated with Gibbs–Helmholtz equation (6) based on urea-unfolding data (continuous lines) and on the temperature induced unfolding (dotted lines) (Table 4). Indicating data points are calculated form the fluorometric urea-unfolding profiles (Figure 6). The difference between the melting temperature of the oxidized and reduced form are indicated (double headed arrows). (b) The thermal denaturation of wild-type and Sa_Trx P31T monitored by DSC.

and enthalpies for the endotherms (Table 4). Removing the proline results in a drop of $\Delta(T_{1/2})_{ox/red}$ from 15.5 °C (wild-type) to 5.8 °C (P31T mutant).

Urea-induced unfolding

Chemical unfolding of the oxidized and reduced forms of Sa_Trx gives similar thermodynamic parameters as temperature unfolding (compare the continuous and dotted lines in Figure 5(a); Table 4). The oxidized form is more stable than the reduced form and stability difference between the oxidized and reduced form decreases when the active site proline is replaced by a threonine (compare the difference between the red and the black lines in Figure 6).

We monitored urea-induced unfolding of oxidized and reduced wild-type Sa_Trx and the P31T mutant by measuring the intrinsic fluorescence spectra upon excitation at 275 nm. Residues that contribute to the emission spectra are tyrosine and tryptophan residues. Sa_Trx contains two tryptophan residues, W28 and W25, rather exposed to the bulk solvent in the folded state and two tyrosine residues, Y46 and Y67, of which Y67 is fairly buried.

The fluorescence spectra of wild-type Sa_Trx and the P31T mutant were similar. As such, we only discuss the results obtained for oxidized and reduced wild-type at one single temperature (Figure 7). In the folded state of oxidized wild-type Sa_Trx, the signal for the tryptophan is completely quenched by the presence of the disulfide bridge in the active site,[23] and the barely detectable emission maximum of tyrosine at 308 nm becomes visible. In the reduced form (Figure 7), we observe a red shift of the emission maximum of about 5 nm between the folded and unfolded state. The already surface-exposed tryptophan residues go to an even more polar environment upon unfolding. The difference spectrum between the folded and unfolded states shows a maximum at 356 nm for oxidized and 358 nm for reduced Sa_Trx. For both oxidized and reduced states of wild-type and mutant Sa_Trx, the unfolding was completely reversible, as checked by

Table 4. Redox state dependent thermodynamic parameters of Sa_Trx obtained from the model analysis of DSC endotherms and the fluorometric urea unfolding profiles

Sa_Trx variant	Redox state	$T_{1/2}$ (°C)		ΔC_p^o (kcal/mol/°C)		ΔH_{vh} ($T_{½}$) (kcal/mol)		ΔH_c ($T_{½}$) (kcal/mol)	$\Delta H_c/\Delta H_{vh}$	$\Delta(T_{1/2})_{ox/red}$ (°C)	
		DSC	Urea	DSC	Urea	DSC	Urea	DSC	DSC	DSC	Urea
Wild-type	Oxidized	73.2	74.5	1.7	1.5	77.7	71.6	72.7	0.93	15.5	18.7
	Reduced	57.6	55.7	1.9	1.9	57.2	57.6	59.3	1.02		
P31T	Oxidized	70.3	69.7	1.9	1.8	72.4	70.4	69.5	0.96	5.8	6.8
	Reduced	64.5	62.9	1.9	2.1	63.9	66.3	63.1	0.99		
Error[a]		±0.4		±0.1		±2.3	±3.2				

[a] The relative parameters errors were estimated from repetitive experiments by variation of possible base-line positions and are higher than those derived from the fitting of the model function to the individual unfolding curves (calculated as square roots of diagonal

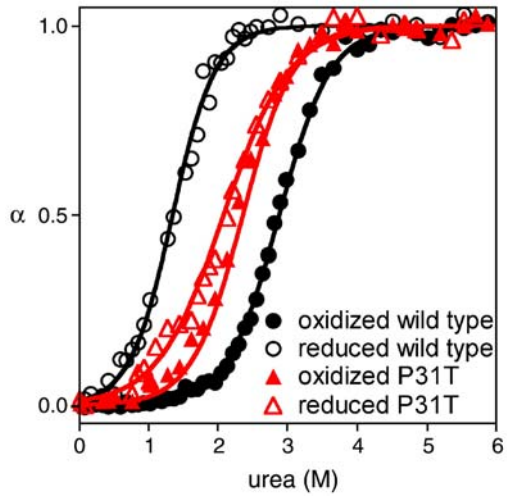

Figure 6. Fraction of unfolding (α) of oxidized (filled symbols) and reduced (open symbols) wild-type Sa_Trx (black) and Sa_Trx P31T (red) at 25 °C as a function of urea concentration. The α value was calculated from equation (4) with data from the fluorescence emission spectra recorded for oxidized and reduced Sa_Trx at 356 nm and 358 nm, respectively (Figure 7).

diluting the sample to pre-transition urea concentrations. A two-state unfolding model consisting of the equilibrium between a folded and unfolded monomer adequately describes the data.

Discussion

Each of the conserved proline residues (Figure 1) in thioredoxin plays a different role. The conserved proline in the α2 helix (P37 in Sa_Trx) is not essential for its redox function (Figures 1 and 3), but stabilizes the protein.[24] The conserved *cis*-proline located on the opposite site of the WCGPC active site motif (P73 in Sa_Trx) is important for maintaining the conformation of the active site and the redox potential of thioredoxin (Figures 1 and 3).[25] Replacing it by an alanine has an effect on the efficiency of catalysis. The conserved active site proline (P31 in Sa_Trx) (Figures 1 and 3) is the key residue that determines the reducing power of thioredoxin. Replacing the proline by a histidine in Ec_Trx increases the redox potential with 35 mV relative to wild-type and the catalytic activity in disulfide reduction decreases.[26] However, it was also shown in Ec_Trx that replacing the active site proline to serine has only a little effect on the redox activity.[19,25] We showed with *S. aureus* thioredoxin that replacing the central proline of the WCGPC active site motif by a serine or a threonine has a gigantic effect. It results in a decrease of the pK_a of the nucleophilic cysteine, an increase in redox potential, a decrease in the efficiency of catalysis, and a decrease in stability difference between the oxidized and reduced form.

The pK_a of the nucleophilic cysteine is not only determined by the WCGPC active site motif, but also by the presence of helix α2, and the side-chains of Asp23, Lys54, and Pro73[27–30] (Figure 2). All these elements are structurally conserved between wild-type and mutant Sa_Trx and therefore seem not responsible for modifying the pK_a of the mutants. The only recognizable difference between wild-type Sa_Trx and the mutants is a change to a more hydrophilic environment around the sulfur of nucleophilic Cys29 by the introduction of a free backbone amine group at position 31 and the conversion of a hydrophobic to a hydrophilic side-chain. No clear hydrogen bonds are introduced. As such, in contradiction to DsbA and Grx,[31,32] the local effect of the central residues of the active site on the pK_a may not be understood in terms of the number of hydrogen bonds that these residues can provide

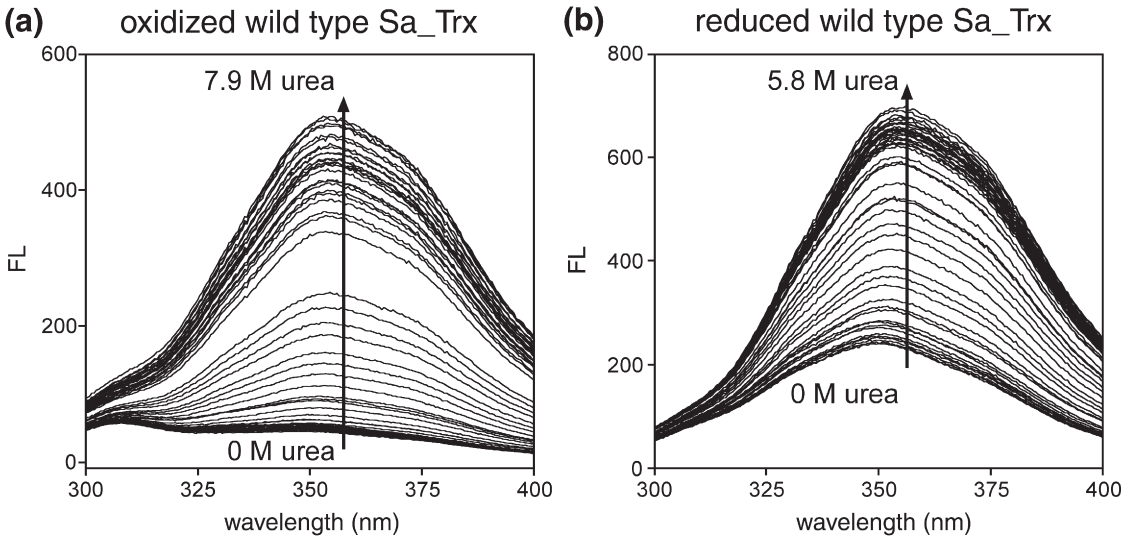

Figure 7. Fluorescence emission spectra for urea-induced unfolding of oxidized (a) and reduced (b) wild-type Sa_Trx measured at 30 °C, pH 7.8.

to stabilize the charge on the nucleophilic thiolate. Although no hydrogen bond interactions were observed in the X-ray structures, it is tempting to speculate that local flexibility might induce hydrogen bond interactions in a short time frame, like for Grx from *E. coli*.[33]

The structure of Sa_Trx reveals a hydrophobic patch close to the accessible nucleophilic cysteine region, consisting of W25, A26 and W28 (Figure 2). Multiple sequence alignment reveals that A26 and W28 are conserved in the thioredoxin family (Figure 1). The indole side-chain of Trp28 is turned towards the interior of the protein and covers an important part of the active site surface (Figure 2). This particular positioning of the indole side-chain is not due to the crystal packing, since the same position is observed in the solution structures of Ec_Trx (PDB code entries 1XOA, 1XOB).[4] The indole ring of Trp28 is in van–der Waals contact with the conserved Ala26–methyl group. There are no direct interactions of Trp28 with the nucleophilic Cys29. Trp28 interacts with Asp58 ($W28N^{\varepsilon 1}$–$D58O^{\delta 1}$: 3.3 Å and $W28N^{\varepsilon 1}$–$D58O^{\delta 2}$: 2.6 Å) and with Ala26 ($N^{\varepsilon 1}$–C^{β}: 3.3 Å) (Figure 3).

Although no interaction with the nucleophilic cysteine is observed, the presence of this conserved active site tryptophan (Figure 3) keeps the pK_a of this cysteine low and favours the thiolate anion form in thioredoxin h from *Chlamydomonas reinhardtii*.[34] The electron-rich indole ring in the vicinity of a thiol might act as a base to help the thiol to deprotonate. In the structure of *C. reinhardtii* thioredoxin h,[35] the Trp to Ala mutation results in an increased solvent exposure of the nucleophilic cysteine with an increased pK_a as a consequence.

We could confirm these results with a W28A mutant of *S. aureus* thioredoxin, the pK_a of the nucleophilic cysteine increases to a value typical for a free thiol, i.e. 8.3(±0.1) and its redox potential decreases to −284(±6) mV. Replacing the bulky indole side-chain of the tryptophan by a methyl group structurally destabilises Sa_Trx in such a way that it shows a strong tendency to form multimers and shows the characteristics of a partially unfolded population (unpublished results).

The correlation between a decreasing redox potential and an increasing pK_a is expected from the theory of Szajewski and Whitesides, which predicts the rate constants of disulfide exchange reactions from the pK_a values of all involved thiols.[36] When the redox potential increases, the pK_a of the nucleophilic cysteine decreases. Wild-type, P31T, P31S Sa_Trx, and even DsbA, follow the predicted correlation, which results in a slope of −42(±3) mV/pH unit (r^2 = 0.99) (Figure 8). The Sa_Trx W28A mutant is an outliner. Adding Sa_Trx W28A in this series, r^2 drops to 0.94 and as such, the effect of the W28A mutation is not translated into a similar redox potential *versus* pH slope. Not a surprise, taken the molten-globule like behaviour of this mutant into account.

What exactly links the stability of the oxidized and reduced forms of Sa_Trx with disulfide bond reduction? Thioredoxin most likely reacts with glutathione according to the following scheme:

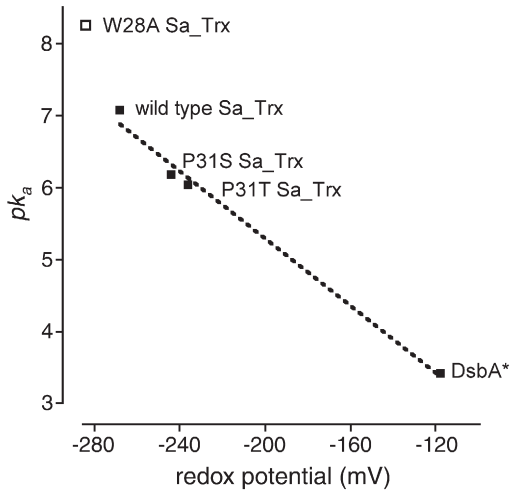

Figure 8. The redox potential of the active site cysteine residues correlates with the pK_a of the nucleophilic cysteine. The redox potential decreases with 42.3 mV per pH unit (r^2 = 0.99). The *DsbA value was obtained from Grauschopf *et al.*[31]

$$Trx_{(SH)_2} + GSSG \rightleftharpoons TrxSSG + GSH \rightleftharpoons Trx_{(ss)} + 2GSH.$$

TrxSSG represents the mixed disulfide formed between glutathione and Sa_Trx. This scheme might be considered as a model for any disulfide containing substrate. Since the oxidized form of wild-type Sa_Trx is far more stable than the reduced form over the whole temperature range (Figure 5(a)), the equilibrium of the reaction is driven to the right and *GSSG* is being reduced. The pK_a of the nucleophilic cysteine makes the thiolate unstable at neutral pH and allows thioredoxin to form mixed disulfide bonds with substrate proteins through a thermodynamically driven reaction towards the oxidized form. For the natural oxidase DsbA the opposite is true.[31] Here, a low pK_a of its nucleophilic cysteine and a higher stability of reduced form compared to the oxidized one establish DsbA's oxidizing power.

In P31T Sa_Trx, a more hydrophilic chemical surrounding of the nucleophilic cysteine results in a decreased pK_a of Cys29 (Table 2; Figure 4(a)) and makes the thiolate more reactive. However, the decreased difference in stability between the oxidized and reduced form compared to wild-type (Figure 5(a)), makes from this P31T mutant a less reducing agent. This was clearly observed with oxidized arsenate reductase as a substrate. This mutation has no effect on substrate recognition (the K_M has not changed compared to wild-type), but the rate of disulfide reduction (k_{cat}) is about seven times lower compared to wild-type Sa_Trx (Table 3).

According to our knowledge this is the first time that the stability of oxidized and reduced thioredoxin were analysed with temperature and chemical unfolding over the whole temperature range (Figure 5(a)). In general, wild-type Sa_Trx is less stable

compared to wild type Ec_Trx. Oxidized Ec_Trx has a $\Delta G^{\circ}_{H_2O,T}$ of 9.9 kcal/mol (obtained with GdmHCl induced unfolding at 25 °C, pH 7.0)[37] and a $T_{1/2}$ of 90 °C.[38] Oxidized Sa_Trx displays at 25 °C a $\Delta G^{\circ}_{H_2O,T}$ of 4.6 kcal/mol and a $T_{1/2}$ of 74.5 °C (Figure 5(a); Table 4). At the same temperature, reduced Ec_Trx has a $\Delta G^{\circ}_{H_2O,T}$ of 5.8 kcal/mol,[37] while reduced Sa_Trx displays a $\Delta G^{\circ}_{H_2O,T}$ of 2.6 kcal/mol (Figure 5(a)). Based on the stability differences at 25 °C, these data strongly suggest that Ec_Trx is not only more stable than Sa_Trx, but is also a better reducing agent than Sa_Trx.

In conclusion, this study reveals two features of thioredoxin that explains its reducing behaviour: the large stabilization of the oxidized form, and the relatively high pK_a of its nucleophilic cysteine compared to the oxidase DsbA. We have stressed the importance of the presence of a conserved proline in the WCGPC motif to keep the $\Delta(T_{1/2})_{ox/red}$ value high enough to drive the reduction reaction to completion. Mutation of the conserved proline alters the redox properties of Sa_Trx in a predictable way: stabilisation of the thiolate on the nucleophilic cysteine shifts the equilibrium more towards the reduced form, by which thioredoxin becomes a more oxidizing agent. Therefore, the idea first suggested by Krause *et al*.[39] and later on explored by Mossner *et al*.[37] that a thioredoxin can be converted to an oxidant or reductant by rational means, is extended. As such, the evolutionary choice of a proline in active site determines the redox properties of thioredoxin as reducing agent.

Material and Methods

Site-directed mutagenesis, expression, purification and crystallization of wild-type and mutant Sa_Trx

Sa_Trx mutants for crystallization were constructed, expressed and purified as described.[40,41] A pET-14b vector containing the wild type *trxA* gene[40] was used as DNA template in PCR amplification with primers designed to introduce the C32A mutation. The resulting PCR fragments were digested with NdeI and BamHI, cloned into the pET-14b vector (Novagen, Madison, WI), transformed in *E. coli* strain BL21 (DE3). For crystallization trials, the cleavable N-terminal His-tag was removed, but for DSC experiments as well as redox potential and pK_a determination it was retained.

Crystal structure determination

Crystallization and X-ray data collection have been reported.[41] The structures were determined by molecular replacement using Amore[42] with *Alicyclobacillus acidocaldarius* thioredoxine (40% sequence identity) as starting model (PDB entry 1NW2). Refinement against structure factor amplitudes was done using the maximum likelihood function of CNS 1.0.[43] Bulk solvent and anisotropic *B* factor corrections were used throughout the refinement. After an initial rigid body refinement followed by a slow cool stage, electron density maps were generated and the model was rebuilt manually with the graphics program TURBO.[44] From then on rounds of refinement of atomic positions and individual *B*-factors were alternated with model building until no further improvement could be obtained.

The final coordinates of the wild-type structure were then used as starting model for refinement against the data of the mutant proteins using the same protocol as described above. The structures were controlled on their quality with PROCHECK.[45]

Determination of the redox potential

Redox buffer solutions were prepared in a 100 mM potassium phosphate (pH 7.0), 1 mM EDTA. All solutions were de-oxygenated with argon for at least 2 h. The GSH/GSSG redox potential was calculated according to the Nernst equation:

$$E'_h = E^{o'} - \frac{RT}{nF}\ln([GSH]^2/[GSSG]) \quad (1)$$

with $E^{0'} = -240$ mV at pH 7.0 and $n = 2$ for the two-electron oxidation of 2GSH to GSSG. The appropriate molar concentrations of GSH and GSSG were used to achieve the desired redox potentials (Table 2). Equilibrium was reached after 2 h of incubation of Sa_Trx P31S or P31T at room temperature in different GSH/GSSG mixtures. To determine the amount of reduced Sa_Trx, samples were injected on Vydac C18 column (4.6 mm × 250 mm) (Vydac, Hesperia, CA) equilibrated in 15% (v/v) acetonitrile, 0.1% (v/v) trifluoroacetic acid (TFA) at 1 ml/min. The column was developed with a 25 min linear gradient from 15% to 50% acetonitrile at room temperature. Absorption data collection at 280 nm and peak integration was performed under Empower (Waters, Milford Massachusetts). The percentage reduced Sa_Trx was plotted as a function of the redox potentials (E'_h) to determine the midpoint potential (Figure 4(b)).

Mass spectrometry

The oxidation state of the purified, reduced and oxidized Sa_Trx samples was checked with mass spectrometry. After a reversed-phase chromatography run (*vide supra*), the peak fractions were diluted ten times in a mixture of 50% acetonitrile and 0.1% (v/v) formic acid before analysis by mass spectrometry. The samples were loaded into a nanoflow capillary (Proxeon, Odense, Denmark) and ESI mass spectra were acquired on a quadrupole time-of-flight instrument (Q-Tof Ultima; Micromass/Waters, Manchester, UK) operating in the positive ion mode, equipped with a Z-spray nanoelectrospray source. Capillary voltages of 1.1 kV–1.5 kV and a cone voltage of 50 V were used. The source temperature was kept at 80 °C. The molecular mass of the proteins was determined after processing of the spectra with the MaxEnt1 software (Micromass/Waters).

Determination of the pK_a of the nucleophilic cysteine

The thiolate ion has a higher absorption at 240 nm than the unionised thiolate group, allowing the determination of the thiol pK_a by monitoring UV absorption during pH titration.[21] The pH of a Sa_Trx solution (0.5 mg/ml) was buffered with a poly-buffer solution containing 10 mM sodium citrate, borate and phosphate.

Sa_Trx was first reduced with 100 mM DTT for 15 min at room temperature. As a reference, oxidized Sa_Trx was incubated for 30 min at room temperature with 40 mM diamide. The excess of DTT and diamide were removed on a Superdex75 HR column (GE Healthcare, Uppsala, Sweden) equilibrated with poly-buffer solution at pH 8.5 (for wild-type, P31S, P31T, and P31TC32S Sa_Trx) or pH 9.5 (for C32A Sa_Trx). The redox state of Sa_Trx was checked on a Vydac C18 column (*vide supra*). For titration experiments, 100 mM HCl was added stepwise to the Sa_Trx solution in portions of 20 μl to 50 μl. The absorbance at 280 nm and 240 nm was recorded on a Cary 100 Bio UV-visible spectrophotometer (Varian, Palo Alto, CA). As the absorbance of Sa_Trx at 280 nm was proved to be pH independent (A_{240red}/A_{280red})/(A_{240ox}/A_{280ox}) was used as a measure of the fraction of the Cys29 thiolate. The pH dependent absorption was fitted (Figure 4(a)) according to the Henderson–Hasselbach equation:

$$A_{exp} = A_{SH} + \frac{(A_{S^-} - A_{SH})}{1 + 10^{(pKa-pH)}} \quad (2)$$

in which A_{exp} is A_{240}/A_{280} for the experimental determined value, A_{SH} is the A_{240}/A_{280} value for the protonated form and A_{S^-} is the A_{240}/A_{280} for deprotonated form.

Kinetic assays

The Michaelis–Menten kinetic parameters were determined under the assay conditions as described.[6] To determine the efficiency of thioredoxin recognition by thioredoxin reductase, 100 μM of Sa_Trx wild-type, P31T and P31S were used as substrate for 0.2 μM of thioredoxin reductase in the presence of 500 μM NADPH in the same buffer solution and assay conditions as described.[6]

Fluorescence spectroscopy

The unfolding of wild-type and mutants of Sa_Trx was induced in 0–7.9 M urea (high purity–enzyme grade; Rose Chemicals, London, UK). Fluorescence emission spectra were recorded on a LS 55 luminescence spectrometer (Perkin Elmer, Wellesley) equipped with a thermally controlled cell holder and a cuvette with a 10 mm path length. Urea-induced unfolding was measured using the changes in intrinsic emission fluorescence between 300 nm and 400 nm upon excitation at 275 nm. The measurements were performed at different temperatures, varying from 10 °C to 55 °C, in 50 mM sodium phosphate (pH 7.8). Each sample contained 2.8 μM–5 μM of protein and reduced samples additionally contained 2.5 mM DTT. Samples were incubated at least 4 h before the measurements in order to achieve equilibrium. The reversibility of the unfolding transitions was checked by diluting the samples from 7.9 M urea to pre-transition urea concentrations and re-scanning the emission spectrum. All urea-induced unfolding curves were analysed by fitting the two state unfolding model $N \overset{K}{\leftrightarrow} D$ to the experimental data.

Differential scanning calorimetry (DSC)

All calorimetric scans were performed using a MicroCal VP-DSC high-sensitivity differential scanning microcalorimeter with a 0.515 ml cell. Three different scanning rates were used: 1.5, 1 and 0.5 K/min. The protein concentration used in the experiments was 0.5–1.0 mg/ml. The samples were always filtered and degassed for 10 min at 283 K before being examined in the calorimeter. The reversibility of thermally induced transitions was checked by re-heating the solution in the calorimeter cell after cooling from the up-scan run. For the oxidized proteins, the buffer used in the calorimetric experiments was 50 mM sodium phosphate (pH 7.0), 200 mM NaCl. In the case of the reduced forms, 50 mM of DTT was required to guarantee complete reduction.

To obtain the thermograms (C_p–$C^o_{p,N}$ *versus* T curves), the heat capacity of the protein in the initial (folded) state was subtracted from the raw signal corrected for the buffer contribution.

Analysis of thermal and urea-induced unfolding data

All the calorimetric data were analysed using the MicroCal Origin DSC 7.0 software package assuming a two-state process:

$$N \overset{K}{\leftrightarrow} D \quad K = \frac{\alpha}{(1-\alpha)} = e^{\frac{-\Delta G^o_T}{RT}} \quad (3)$$

where K is the equilibrium denaturation constant, and R is the universal gas constant and α is the fraction of protein in the denatured state that depends on the temperature or denaturant concentration, respectively. According to this model, one can express an average of a physical property, θ (in our case, θ is the partial molar enthalpy of the protein or the fluorescence intensity (FL)), in terms of the corresponding contributions θ_N and θ_D, which characterize native (N) and denatured (D) states, respectively.[46]

$$\theta = \theta_N + \alpha \cdot (\theta_D - \theta_N) \quad (4)$$

For the transitions followed by fluorescence, θ_N and θ_D are assumed to be linear functions of the concentration of urea. The model function C_p–$C^o_{p,N}$ for the DSC signal is the partial molar heat capacity of the protein relative to state N. It can be derived from the first partial derivative of equation (4) on temperature at constant pressure:[47,48]

$$C_p - C^o_{p,N} = \alpha \Delta C^o_p + \frac{\alpha(1-\alpha)}{RT^2}\left[\Delta H^o_{T_{1/2}} + \Delta C^o_p (T - T_{1/2})\right]^2 \quad (5)$$

The thermodynamic parameters that characterize the melting curves ($\Delta H^o_{T_{1/2}}$, ΔC^o_p and $T_{1/2}$) were obtained by fitting the model function for DSC to the experimental temperature profiles using the Levenberg–Marquardt non-linear χ^2 regression procedure.[49]

The conformational stability of a protein that unfolds in a two-state fashion, expressed in terms of the corresponding standard free energy change, ΔG^o_T, can be obtained by applying the Gibbs–Helmholtz equation:

$$\Delta G^o_T = T[\Delta H^o_{T_{1/2}}(1/T - 1/T_{1/2}) + \Delta C^o_p(1 - T_{1/2}/T - \ln(T/T_{1/2}))] \quad (6)$$

In this expression $T_{1/2}$ is the melting temperature at which $\alpha = 0.5$, $\Delta H^o_{T_{1/2}}$ is the standard enthalpy of denaturation at $T_{1/2}$, and ΔC^o_p is the difference in heat capacity between the folded and unfolded state assumed to be temperature independent.

The urea-induced unfolding profiles at a given temperature were described by equations (3) and (4) combined with the empirical relation $\Delta G^{o}_{T}=\Delta G^{o}_{H_2O,T}-m[urea]$. Here, $\Delta G^{o}_{H_2O,T}$ is the standard Gibbs free energy of unfolding in the absence of denaturant and m is a proportionality coefficient. These values were then fitted to equation (6) using the χ^2 regression procedure mentioned above to extract the thermodynamic parameters $\Delta H^{o}_{T_{1/2}}$, ΔC^{o}_{P} and $T_{1/2}$ in the absence of denaturant.

Protein Data Bank entry codes

The atomic coordinates and structure factors have been deposited with the RCSB Protein Data Bank, with entry codes 2O7K (Sa_Trx wild-type), 2O85 (Sa_Trx P31T), 2O87 (Sa_Trx P31S) and 2O89 (Sa_Trx P31TC32S).

Acknowledgements

The authors thank Dr Jean-Marie Ruysschaert (Center of Structural Biology and Bioinformatics) for critically reading the manuscript. Onderzoeksraad-Vrije Universiteit Brussel and FWO-Vlaanderen supported this work. The authors acknowledge the use of synchrotron beamtime at the EMBL beamlines at the DORIS storage ring (Hamburg, Germany) and the ESRF (Grenoble France). G. V. gratefully acknowledges the Communauté Française de Belgique (ARC) for financial support.

References

1. Holmgren, A. (1979). Thioredoxin catalyzes the reduction of insulin disulfides by dithiothreitol and dihydrolipoamide. *J. Biol. Chem.* **254**, 9627–9632.
2. Holmgren, A. (1976). Hydrogen donor system for *Escherichia coli* ribonucleoside-diphosphate reductase dependent upon glutathione. *Proc. Natl Acad. Sci. USA*, **73**, 2275–2279.
3. Cha, M. K., Kim, H. K. & Kim, I. H. (1995). Thioredoxin-linked "thiol peroxidase" from periplasmic space of *Escherichia coli*. *J. Biol. Chem.* **270**, 28635–28641.
4. Jeng, M. F., Campbell, A. P., Begley, T., Holmgren, A., Case, D. A., Wright, P. E. & Dyson, H. J. (1994). High-resolution solution structures of oxidized and reduced *Escherichia coli* thioredoxin. *Structure*, **2**, 853–868.
5. Eklund, H., Gleason, F. K. & Holmgren, A. (1991). Structural and functional relations among thioredoxins of different species. *Proteins: Struct. Funct. Genet.* **11**, 13–28.
6. Messens, J., Van Molle, I., Vanhaesebrouck, P., Limbourg, M., Van Belle, K., Wahni, K. *et al.* (2004). How thioredoxin can reduce a buried disulphide bond. *J. Mol. Biol.* **339**, 527–537.
7. Aslund, F., Berndt, K. D. & Holmgren, A. (1997). Redox potentials of glutaredoxins and other thiol-disulfide oxidoreductases of the thioredoxin superfamily determined by direct protein-protein redox equilibria. *J. Biol. Chem.* **272**, 30780–30786.
8. Zapun, A., Bardwell, J. C. & Creighton, T. E. (1993). The reactive and destabilizing disulfide bond of DsbA, a protein required for protein disulfide bond formation *in vivo*. *Biochemistry*, **32**, 5083–5092.
9. Kallis, G. B. & Holmgren, A. (1980). Differential reactivity of the functional sulfhydryl groups of cysteine-32 and cysteine-35 present in the reduced form of thioredoxin from *Escherichia coli*. *J. Biol. Chem.* **255**, 10261–10265.
10. Dyson, H. J., Tennant, L. L. & Holmgren, A. (1991). Proton-transfer effects in the active-site region of *Escherichia coli* thioredoxin using two-dimensional ^{1}H NMR. *Biochemistry*, **30**, 4262–4268.
11. Chivers, P. T., Prehoda, K. E., Volkman, B. F., Kim, B. M., Markley, J. L. & Raines, R. T. (1997). Microscopic pK_a values of *Escherichia coli* thioredoxin. *Biochemistry*, **36**, 14985–14991.
12. Holmgren, A. (1984). Enzymatic reduction-oxidation of protein disulfides by thioredoxin. *Methods Enzymol.* **107**, 295–300.
13. Holmgren, A. (1985). Thioredoxin. *Annu. Rev. Biochem.* **54**, 237–271.
14. Messens, J., Hayburn, G., Desmyter, A., Laus, G. & Wyns, L. (1999). The essential catalytic redox couple in arsenate reductase from *Staphylococcus aureus*. *Biochemistry*, **38**, 16857–16865.
15. Bairoch, A. & Apweiler, R. (1999). The SWISS-PROT protein sequence data bank and its supplement TrEMBL in 1999. *Nucl. Acids Res.* **27**, 49–54.
16. Edman, J. C., Ellis, L., Blacher, R. W., Roth, R. A. & Rutter, W. J. (1985). Sequence of protein disulphide isomerase and implications of its relationship to thioredoxin. *Nature*, **317**, 267–270.
17. Bennett, C. F., Balcarek, J. M., Varrichio, A. & Crooke, S. T. (1988). Molecular cloning and complete amino-acid sequence of form-I phosphoinositide-specific phospholipase C. *Nature*, **334**, 268–270.
18. Katti, S. K., LeMaster, D. M. & Eklund, H. (1990). Crystal structure of thioredoxin from *Escherichia coli* at 1.68 Å resolution. *J. Mol. Biol.* **212**, 167–184.
19. Gleason, F. K., Lim, C. J., Gerami-Nejad, M. & Fuchs, J. A. (1990). Characterization of *Escherichia coli* thioredoxins with altered active site residues. *Biochemistry*, **29**, 3701–3709.
20. Kelley, R. F. & Richards, F. M. (1987). Replacement of proline-76 with alanine eliminates the slowest kinetic phase in thioredoxin folding. *Biochemistry*, **26**, 6765–6774.
21. Nelson, J. W. & Creighton, T. E. (1994). Reactivity and ionization of the active site cysteine residues of DsbA, a protein required for disulfide bond formation *in vivo*. *Biochemistry*, **33**, 5974–5983.
22. Gilbert, H. F. (1990). Molecular and cellular aspects of thiol-disulfide exchange. *Adv. Enzymol. Relat. Areas Mol. Biol.* **63**, 69–172.
23. Holmgren, A. (1972). Tryptophan fluorescence study of conformational transitions of the oxidized and reduced form of thioredoxin. *J. Biol. Chem.* **247**, 1992–1998.
24. de Lamotte-Guery, F., Pruvost, C., Minard, P., Delsuc, M. A., Miginiac-Maslow, M., Schmitter, J. M. *et al.* (1997). Structural and functional roles of a conserved proline residue in the alpha2 helix of *Escherichia coli* thioredoxin. *Protein Eng.* **10**, 1425–1432.
25. Gleason, F. K. (1992). Mutation of conserved residues in *Escherichia coli* thioredoxin: effects on stability and function. *Protein Sci.* **1**, 609–616.
26. Lundstrom, J., Krause, G. & Holmgren, A. (1992). A Pro to His mutation in active site of thioredoxin increases its disulfide-isomerase activity 10-fold. New refolding systems for reduced or randomly oxidized ribonuclease. *J. Biol. Chem.* **267**, 9047–9052.

27. Chivers, P. T., Prehoda, K. E. & Raines, R. T. (1997). The CXXC motif: a rheostat in the active site. *Biochemistry*, **36**, 4061–4066.
28. Dyson, H. J., Jeng, M. F., Tennant, L. L., Slaby, I., Lindell, M., Cui, D. S. *et al.* (1997). Effects of buried charged groups on cysteine thiol ionization and reactivity in *Escherichia coli* thioredoxin: structural and functional characterization of mutants of Asp 26 and Lys 57. *Biochemistry*, **36**, 2622–2636.
29. Kortemme, T. & Creighton, T. E. (1995). Ionisation of cysteine residues at the termini of model alpha-helical peptides. Relevance to unusual thiol pK_a values in proteins of the thioredoxin family. *J. Mol. Biol.* **253**, 799–812.
30. Jacobi, A., Huber-Wunderlich, M., Hennecke, J. & Glockshuber, R. (1997). Elimination of all charged residues in the vicinity of the active-site helix of the disulfide oxidoreductase DsbA. Influence of electrostatic interactions on stability and redox properties. *J. Biol. Chem.* **272**, 21692–21699.
31. Grauschopf, U., Winther, J. R., Korber, P., Zander, T., Dallinger, P. & Bardwell, J. C. (1995). Why is DsbA such an oxidizing disulfide catalyst? *Cell*, **83**, 947–955.
32. Foloppe, N. & Nilsson, L. (2004). The glutaredoxin -C-P-Y-C- motif: influence of peripheral residues. *Structure*, **12**, 289–300.
33. Foloppe, N., Sagemark, J., Nordstrand, K., Berndt, K. D. & Nilsson, L. (2001). Structure, dynamics and electrostatics of the active site of glutaredoxin 3 from *Escherichia coli*: comparison with functionally related proteins. *J. Mol. Biol.* **310**, 449–470.
34. Krimm, I., Lemaire, S., Ruelland, E., Miginiac-Maslow, M., Jaquot, J. P., Hirasawa, M. *et al.* (1998). The single mutation Trp35→Ala in the 35–40 redox site of *Chlamydomonas reinhardtii* thioredoxin h affects its biochemical activity and the pH dependence of C36–C39 ^{1}H-^{13}C NMR. *Eur. J. Biochem.* **255**, 185–195.
35. Menchise, V., Corbier, C., Didierjean, C., Saviano, M., Benedetti, E., Jacquot, J. P. & Aubry, A. (2001). Crystal structure of the wild-type and D30A mutant thioredoxin h of *Chlamydomonas reinhardtii* and implications for the catalytic mechanism. *Biochem. J.* **359**, 65–75.
36. Szajewski, R. & Whitesides, G. (1980). Rate constants and equilibrium constants for thiol-disulfide interchange reactions involving oxidized glutathione. *J. Am. Chem. Soc.* **102**, 2011–2026.
37. Mossner, E., Huber-Wunderlich, M. & Glockshuber, R. (1998). Characterization of *Escherichia coli* thioredoxin variants mimicking the active-sites of other thiol/disulfide oxidoreductases. *Protein Sci.* **7**, 1233–1244.
38. Perez-Jimenez, R., Godoy-Ruiz, R., Ibarra-Molero, B. & Sanchez-Ruiz, J. M. (2005). The effect of charge-introduction mutations on *E. coli* thioredoxin stability. *Biophys. Chem.* **115**, 105–107.
39. Krause, G., Lundstrom, J., Barea, J. L., Pueyo de la Cuesta, C. & Holmgren, A. (1991). Mimicking the active site of protein disulfide-isomerase by substitution of proline 34 in *Escherichia coli* thioredoxin. *J. Biol. Chem.* **266**, 9494–9500.
40. Messens, J., Martins, J. C., Brosens, E., Van Belle, K., Jacobs, D. M., Willem, R. & Wyns, L. (2002). Kinetics and active site dynamics of *Staphylococcus aureus* arsenate reductase. *J. Biol. Inorg. Chem.* **7**, 146–156.
41. Roos, G., Brosens, E., Wahni, K., Desmyter, A., Spinelli, S., Wyns, L. *et al.* (2006). Combining site-specific mutagenesis and seeding as a strategy to crystallize "difficult" proteins: the case of *Staphylococus aureus* thioredoxin. *Acta Crystallog. sect. F*, **62**, 1255–1258.
42. Navaza, J. (1994). Amore. *Acta Crystallog. sect. A*, **50**, 157–163.
43. Brunger, A. T., Adams, P. D., Clore, G. M., DeLano, W. L., Gros, P., Grosse-Kunstleve, R. W. *et al.* (1998). Crystallography and NMR system: a new software suite for macromolecular structure determination. *Acta Crystallog. sect. D, Bi54, 905–921.*
44. Roussel, A. & Cambillau, C. (1989). *TURBO-FRODO in Silicon Graphic Geometry Partner Directory.* Silicon Graphics, Mountain View, CA.
45. Laskowski, R. A., MacArthur, M. W., Moss, D. S. & Thornton, J. M. (1993). PROCHECK: a program to check the stereochemical quality of protein structures. *J. Appl. Crystallog.* **26**, 283–291.
46. Pace, C. N. (1986). Determination and analysis of urea and guanidine hydrochloride denaturation curves. *Methods Enzymol.* **131**, 266–280.
47. Lopez, M. M. & Makhatadze, G. I. (2002). Differential scanning calorimetry. *Methods Mol. Biol.* **173**, 113–119.
48. Freire, E. & Biltonen, R. L. (1978). Statistical mechanical deconvolution of thermal transitions in macromolecules. I. Theory and application to homogeneous systems. *Biopolymers*, **17**, 463–479.
49. Press, W. H. & Vetterling, W. T. (1992). In *Numerical Recipes in C: The Art of Scientific Computing*. 2nd edit., vol. 2. Cambridge University Press, Cambridge.

Edited by P. Wright

(Received 29 December 2006; received in revised form 10 February 2007; accepted 13 February 2007)
Available online 22 February 2007